

# Photovoltaic micro-inverter with high voltage gain DC-DC converter

Jinsa B Salim, Aabida C A

**Abstract**— The grid-connected AC module is an alternative solution in photovoltaic (PV) generation systems. It combines a PV panel and a micro-inverter connected to grid. If a low voltage source is used, however, a high gain, high efficiency power conversion stage is required to feed the dc-ac stage used to interface with the AC grid. Such systems, referred to as micro-inverters or module integrated inverters, have become quite popular in recent times. This paper presents a high voltage gain, high efficiency dc-dc converter suitable for micro-inverter application is proposed. Micro-inverters are grid connected systems, which shut down in the event of grid failure. For residential as well as small commercial applications, this can be discouraging as no power is available during grid failure. The proposed inverter includes a high step-up DC-DC converter and a H-bridge inverter. It transfers solar energy into sinusoidal voltage waveform. A controller is used to achieve the system starting check, abnormal state detection, and maximum power point tracking as well as islanding detection.

**Index Terms**— High step-up voltage gain, Photovoltaic(PV), Maximum power point (MPPT) and hybrid pulsewidth modulation.

## I. INTRODUCTION

RENEWABLE energy is becoming increasingly important and prevalent in distribution systems, which provide different choices to electricity consumers whether they receive power from the main electricity source or in forming a microsource not only to fulfill their own demand but alternatively to be a power producer supplying a microgrid. A microgrid usually includes various microsourses and loads, which operate as an independent and controllable system when they are either grid-connected or islanded, as well as when they can reliably connect or disconnect. The microsource is classified either as a dc source or as a high frequency ac source. These two microsource categories are comprised of diverse renewable energy applications, such as solar cell modules, fuel cell stacks, wind turbines, and reciprocating engines.

Conventional photovoltaic (PV) generation system is sourced from several serially connected PV module strings, which provides a sufficiently high voltage which can be converted to electricity through the PV inverter. If there is one or more solar panels in series is/are shaded, changes in output characteristics called 「shading effect」 will occur [1][2]. Any type of shade such as dust, bird droppings, leaves shade, and building shadows will make the output power of solar power system declined dramatically when shade appears, or even caused the system shut down. When one of the PV modules is affected by shade seriously, the output current will decrease immediately and cause the change in output power. It will generate multiple maximum power points and will cause error detection problems. However, when parallel connected PV modules encounter shade, only one maximum power point exists. The MPP detection problem will not happen under the above-mentioned condition, but the output voltage of the module will be too low to transfer energy to grid through the conventional PV inverter, and the large output current will increase the difficulty of system wiring. The micro inverter is used for a single PV module [3]. Because low voltage output is inherent in PV module, a high step-up DC-DC converter is required in the stage before micro inverter. Finally, the solar energy is connected to main grid or electricity through DC-AC inverter. The control circuit not only provides PWM signals to switches of two power stages, but also traces maximum PV module energy as well as real-time grid detection and protection. Fig.1 shows the two-stage micro inverter. The efficiency of conventional boost converter is restricted by duty ratio for higher output voltage. Theoretically, when duty ratio is closed to unity, the voltage gain will be infinity. However, the reverse recovery loss of the output diode and switching losses are large; the equivalent series resistance (ESR) of capacitors and parasitic resistances of inductor also constrained the voltage gain and efficiency [3]-[6].

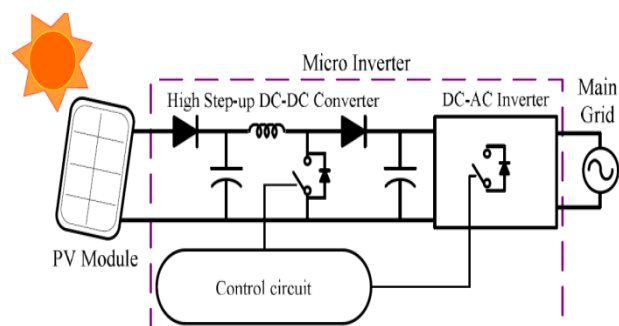


Fig.1 Two stage micro inverter configuration

Manuscript received September, 2015.

Jinsa B Salim, Electrical and Electronics Department, MG University/ KMEA Engineering College., Ernakulam, India.

Aabida C A, Electrical and Electronics Department / KMEA Engineering College, Ernakulam, India

II .DESIGN OF MICRO INVERTER

This paper proposes the design and implementation approach of a PV module micro inverter. The module inverter structure is a two-stage system. The first stage is a high step-up high-efficiency DC-DC converter with maximum power point tracking control. The DC-DC converter raises the input low voltage to a high voltage level, and the maximum power point tracking as well as system starting check control are also achieved in this stage. The second stage is a full-bridge inverter. The DC-AC inverter transforms DC voltage from the first stage into sinusoidal voltage waveform for grid connection, and the abnormal state detection and islanding detection control are also achieved in this stage. The controller is used to achieve 1) the system starting check for the initial settings of the inverter; 2) abnormal state detection on various grid conditions; 3) maximum power point tracking algorithm which uses incremental conductance method; the method senses the output voltage and current of the solar panel to determine the duty cycle of the DC converter to be increased or decreased; 4) frequency shift method is chosen for islanding detection; frequency shift method induces some distortion to the output current of the inverter for controller to detect.

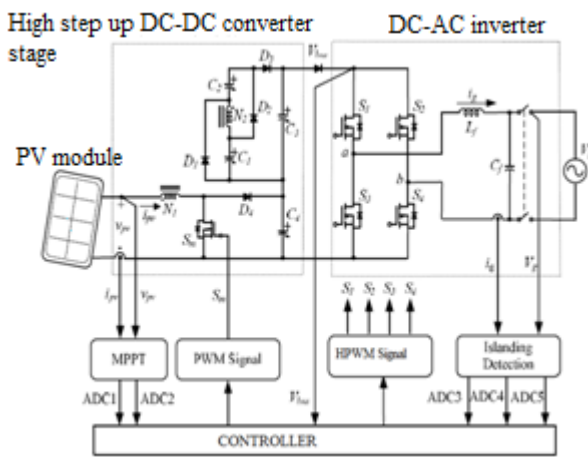


Fig .2 The PV Micro Inverter Structure System in this paper

A. High step-up DC-DC converter stage

The proposed converter has several features: 1) the connection of the two cells, the coupled inductor and the switched-capacitor circuit give a large step-up voltage conversion ratio; 2) the source energy is transferred through the coupled inductor to either the load or switched capacitors during the entire switching period; 3) the leakage inductor energy of the coupled-inductor can be recycled, increasing the efficiency. This also has the benefit of reducing the voltage stress on the active switch.

**Mode I:** In this mode, switch  $S_m$  is turned on, only diode  $D_3$  is conducted. Magnetizing inductor  $L_m$  is storing energy from  $V_{in}$ , and switched capacitors changes their condition from charging to discharging energy to output. The magnetizing inductance  $L_m$  and primary leakage inductance  $L_{k1}$  are storing energy from  $V_{in}$ ; meanwhile  $V_{in}$  is also

transferred through coupled inductor to secondary winding  $N_2$  and be in series with switched capacitor  $C_1$  and  $C_2$ , and then their energy is discharged to capacitor  $C_3$  and load  $R$ . This mode ends when switch  $S_m$  is turned off.

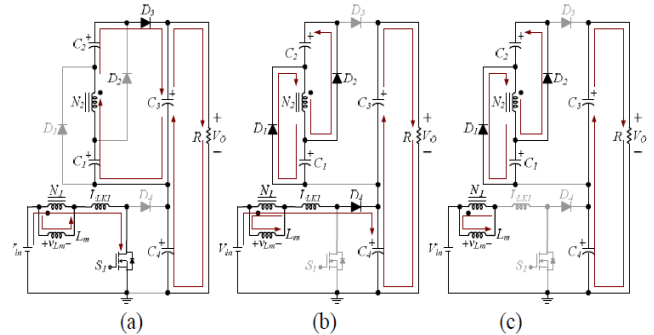


Fig.3 Two Operating modes during one switching period at CCM

**Mode II:** During this transition interval, the  $L_m$  is changed from storing to releasing energy; switched capacitors are also changed from discharging to charging status. Switch  $S_m$ , diodes  $D_1$ ,  $D_2$  and  $D_4$  are conducted. The leakage energy charge capacitor  $C_4$  through diode  $D_4$ ; the  $L_m$  is delivering its energy through coupled inductor to charge capacitor  $C_1$  and  $C_2$ . The mode ends when currents  $i_{Lk1}$  decreased to zero.

**Mode III:** During the interval, The  $L_m$  is constantly releasing its energy to switched capacitors. The  $S_m$ ,  $D_3$ , and  $D_4$  are off; diodes  $D_1$  and  $D_2$  are conducted. The  $i_{Lm}$  is decreasing because the magnetizing inductance energy charges capacitor  $C_1$  and  $C_2$  continuously through the coupled inductor. The energy stored in capacitor  $C_3$  and  $C_4$  are constantly discharged to the load  $R$ . This mode ends when switch  $S_m$  is turned on at the beginning of the next switching period.

To simplify the steady state analysis, the leakage inductances at secondary and primary sides are neglected. Using the voltage-second balance principle, the voltage across magnetizing inductor  $L_m$  can be written as following:

$$\int_0^{DT_s} V_{in} dt + \int_{DT_s}^{T_s} (V_{in} - V_{C4}) dt = 0 \tag{1}$$

$$\int_0^{DT_s} (V_{C1} + V_{C2} - V_{C3}) dt + \int_{DT_s}^{T_s} V_{C1} dt = 0$$

Arranging above equation ,the voltage across capacitor  $C_3$  and  $C_4$  can be shown as:

$$V_{C4} = \frac{1}{1-D} V_{in} \tag{2}$$

$$V_{C3} = \frac{V_{C1} + DV_{C2}}{D} = \frac{n(1+D)}{1-D} V_{in}$$

The output voltage  $V_O$  is the sum of  $V_{C3}$  and  $V_{C4}$ . The voltage gain ratio MCCM can be written as:

$$M_{CCM} = \frac{V_0}{V_{in}} = \frac{1 + (1 + D)n}{1 - D} \quad (3)$$

The boundary normalized magnetizing inductor time constant  $\tau_{LmB}$  can be derived as:

$$\tau_{LmB} = \frac{D(1 - D)^2}{2(1 + 2n)(1 + n + Dn)} \quad (4)$$

**B. DC-AC Inverter stage**

As shown in Fig. 2, The DC-AC inverter consists of a full bridge inverter comprises of four switches and with a lowpass filter. The hybrid pulse width modulation (HPWM) is used for switch driven [7]. The HPWM method uses two different switching frequency signals to drive switches respectively. There are only two of four switches commuted at lower frequency which is equal to grid frequency. Other two switches are driven by the pulse width modulation signals came from the compared result of sinusoid amplitude signal and triangle carrier. Fig.4 shows the HPWM switch driving signals of the full bridge inverter. The operating modes are described as follows:

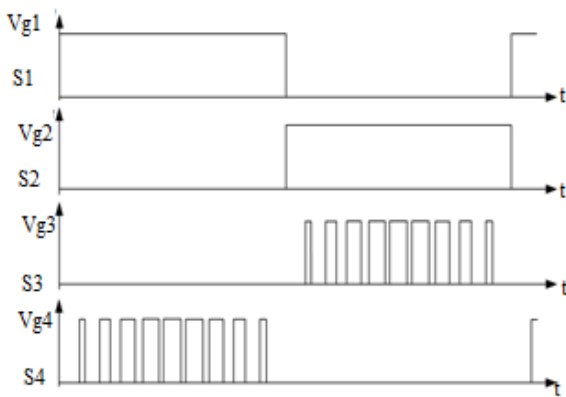


Fig. 4 The HPWM signals on the inverter.

**Mode I:** During positive half cycle, switches *S1* and *S4* are active; other switches including *S2* and *S3* are turned off. The switch *S4* switches of the full-bridge *i* is subject to duty cycle modulation control. The average voltage *vab* among the points *a* and *b* can be derived as:

$$V_{ab} = D V_{bus}$$

The *D* is duty ratio determined by the compared results of the sinusoid amplitude control signal *VControl* and the triangle carrier signal *VTri*. When *VTri* > *VControl*, *S4* is turned on, and vice versa.

**Mode II:** During negative half cycle, switches *S2* and *S3* are active; other switches including *S1* and *S4* are turned off. The switches *S3* is subject to duty cycle modulation control. When *VTri* > *VControl*, *S3* is turned on, the average voltage *vab* among the points *a* and *b* can be derived as:

$$v_{ab} = -D V_{bus}$$

Because of upper switches, *S1* and *S2*, are at commuted at low frequency, the switching losses are significantly reduced than others and the inverter efficiency is then improved [8].

**III. SETTING OF MICRO INVERTER**

There are three major control programs including starting check, system abnormal detection, maximum power point tracking, and islanding detection in the micro inverter. In the following section, the settings and function will be discussed.

**A. Maximum Power Point Tracking Program**

The maximum power point tracking algorithm used in this paper is incremental conductance method [9]-[12]. It senses the PV module output voltage *v<sub>pv</sub>* and current *i<sub>pv</sub>* to determine the duty cycle of the DC-DC step-up converter to be increased or decreased. When the sensed voltage is equal to the voltage from the last cycle and the current increment is positive; then the duty cycle will be increased, and vice versa.

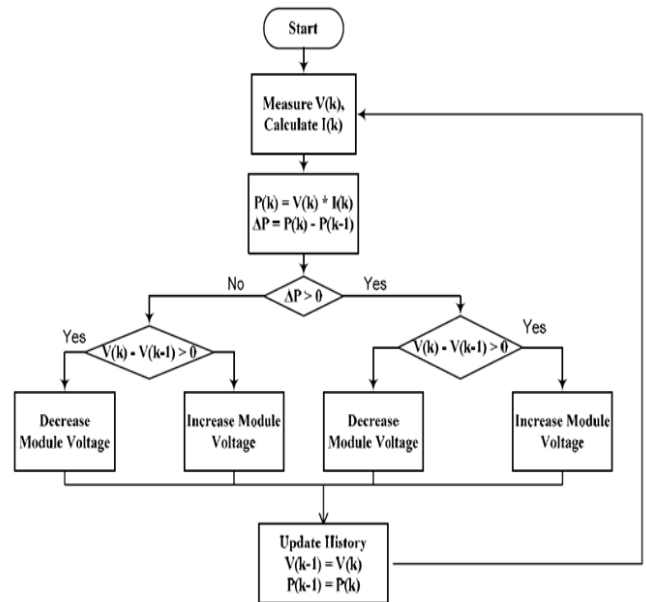


Fig. 5. Maximum power point tracking program flow chart

**B. System Abnormal Protection Program**

The grid voltage range is 88% - 100% of 230 Vrms (194 Vrms – 242 Vrms) and the grid frequency range is 49.3 Hz – 50.5 Hz. When the system abnormal program detects the voltage *v<sub>g</sub>* constantly out of setting range for more than 330ms, or the frequency *f<sub>g</sub>* constantly out of setting range for more than 100ms, the system will be shut down. Fig.6 is the program flow chart of system abnormal detection.

**C. Islanding Detection Program**

The islanding detection is the combination of both active and passive methods. The passive method detects the voltage and frequency changing range as system abnormal detection is working. When the islanding occurs but the abnormal

phenomena are still within the setting range, passive method cannot detect the abnormal condition; therefore the active method is necessary. The active method adopts frequency shift algorithm, which will deform output current waveform.

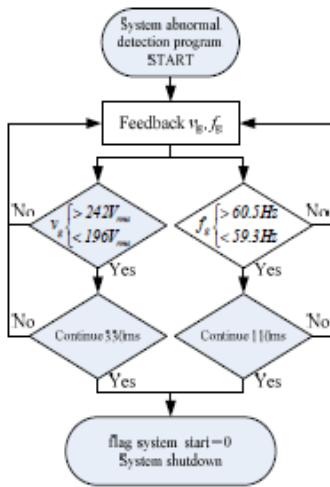


Fig. 6. Abnormal state detection program flow chart

When islanding is occurred, the output current frequency will be shifted, which can be regarded as grid islanding. The system will be shut down immediately.

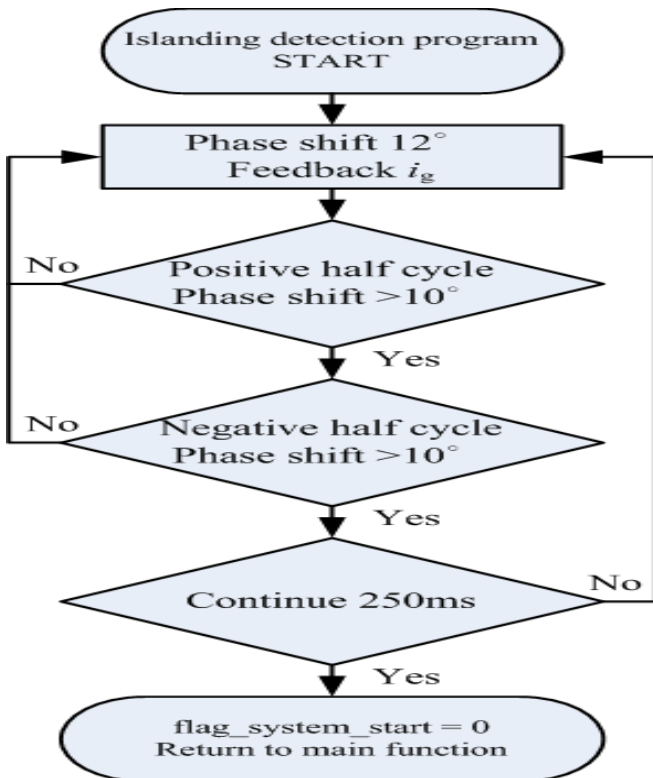


Fig. 7. Islanding detection program flow chart

Total current distortion should be less than 5% and the period of islanding detection time should be within 2 seconds. When the frequency shift is higher than 10° at positive half cycle and negative half cycle, the islanding is triggered. The system will be shut down by the islanding

detection program within 250 ms. Fig.7 is the program flow chart of islanding detection.

IV. SIMULATION RESULTS

Simulations were performed using MATLAB to characterize the behaviour of a prototype of the present invention. The switching frequency for the dc-dc boost converter stage was chosen to be 50 kHz.

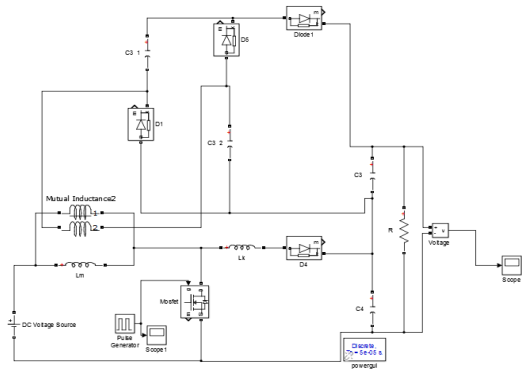


Fig.8 Simulink model of dc-dc converter

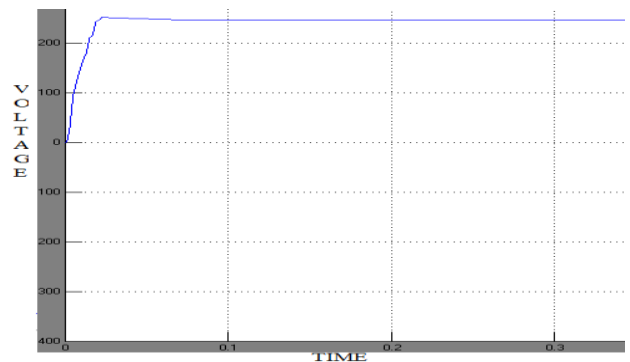


Fig.9 Output voltage DC-DC converter

The typical power rating of a crystalline silicon PV module is 180 W–300 W. A 200 W micro inverter prototype with protection and detection functions is presented to verify the practicability of the proposed micro inverter. Circuit specifications are described as follows: Output power  $PO$  is 200 W; output voltage  $VO$  is 230 VAC; Output frequency  $fO$  is 50 Hz; DC-DC converter output voltage  $VBUS$  is 400 V; Input voltage  $Vpv$  is from 20 to 40 V; Switching frequency  $fm$  of  $Sm$  is 50 kHz; Switching frequency  $fs1$  of  $S1$  and  $S2$  is 120 Hz and Switching frequency  $fs2$  of  $S3$  and  $S4$  is 18 kHz. With reference to [5], the turns ratio is given as  $n = 5$  and the duty ratio  $D$  is about 0.56 for DC-DC step-up converter. When it operates in CCM at half load, the load resistance  $R = 1600 \Omega$ . The actual inductance of magnetizing inductor  $Lm$  of coupled inductor is measured as 18.41  $\mu H$  and the primary leakage inductance is 0.62  $\mu H$ . The Fig.11-15 shows the measured results of proposed detection and protection programs. Fig. 11 is the tracking waveforms of the maximum

power point tracking.. The simulator setting parameters are 1) open circuit voltage 33.2 V, 2) short circuit current 8.58 A, 3) maximum power point voltage 26.6 V, and 4) maximum output current 7.9 A, which are cited from a real PV module

TABLE I. Circuit specifications

Item	Specification
Output power, $P_o$	200 W
Output voltage, $V_o$	230V <sub>AC</sub>
Output frequency, $f_o$	50 Hz
DC-DC converter output voltage, $V_{Bus}$	400 V
Input voltage, $V_{pv}$	20 ~ 40 V
Switching frequency $f_m$ of $S_m$	50 kHz
Switching frequency $f_{z1}$ of $S_1$ and $S_2$	120 Hz
Switching frequency $f_{z2}$ of $S_3$ and $S_4$	18 kHz

TABLE II. Part number of major components

Circuit component	Parameters
<i>DC-DC converter Stage</i>	
Switch, $S_m$	IRFB4410 (100 V/75 A)
Diodes, $D_1 \sim D_3$	BYC8-600 (600 V / 8 A)
Diode, $D_4$	MBR30100 (100 V/30 A)
Capacitors, $C_1$ and $C_2$	47 $\mu$ F / 200V
Capacitor, $C_3$	100 $\mu$ F / 450V
Capacitor, $C_4$	470 $\mu$ F / 100V
<i>DC-AC Full bridge inverter Stage</i>	
Switches, $S_1 \sim S_4$	STW45NM50FD (500 V/45 A)
Filter inductance, $L_f$	4 mH
Filter capacitor, $C_f$	1 $\mu$ F / 250 V <sub>AC</sub>

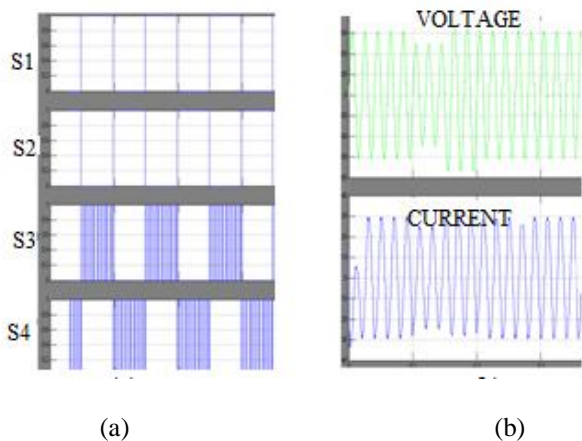


Fig. 10. (a) Four driving signals of switches of the DC-AC inverter. (b) Output voltage and current waveforms as the inverter is connected to grid.

Fig. 11(a) is the tracking record waveforms when the simulator output power is 200 W at the start up of the proposed inverter. Fig. 11(b) is the tracking curves depicts the maximum power point changing from 200 W down to 100 W. The program tracing time is about 400 ms. The

system abnormal protection verification results are depicted in Fig.11 when grid voltage is out of the rated range, which is 194 VAC – 242 VAC, or the grid frequency is out of rated range, which is 49.3 Hz – 50.5 Hz. Fig. 11 (a) illustrates that the system is shut down when the grid voltage is over 242 VAC after 728 ms processing time. Fig. 11(b) shows the

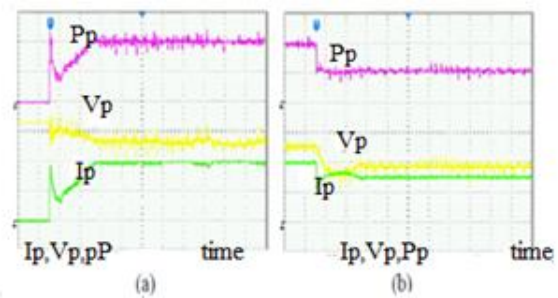


Fig. 11. The measurement waveforms of the maximum power point tracking. (a) Maximum power point under system start up condition. (b) Maximum power point changing from 200 W to 100 W.

system output voltage and current waveforms when the grid voltage is under 196 VAC, and the system is shut down after 696 ms. Fig. 11(c) shows the measured waveforms when the grid frequency is over 50.5 Hz, and the system will be shut down after 150 ms. Fig. 11(d) shows the measured waveforms when the grid frequency is lower than 49.3 Hz, and the system will be shut down after 186 ms. These results show that the abnormal conditions are detected successfully and the system can be shut down within 1 s.

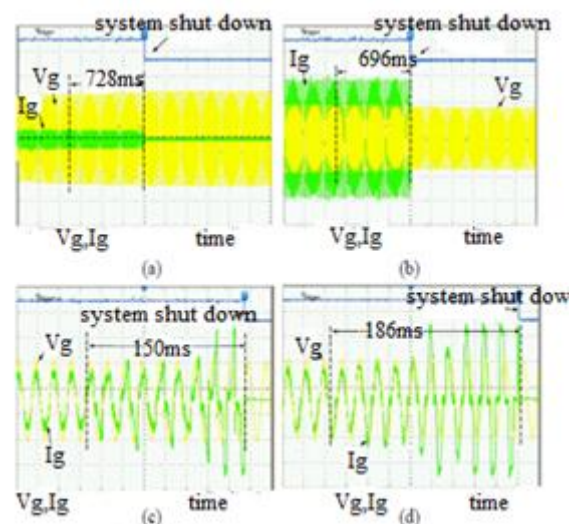


Fig. 12. Measured results of the system when abnormal detection program is activated. (a) The grid voltage is over 242 V. (b) The grid voltage is under 196 V. (c) The grid frequency is over 50.5 Hz. (d) The grid frequency is under 49.3 Hz.

When islanding is occurred or the power grid is disconnected, the islanding protection program will be activated. Fig. 13(a) shows the phase shift scheme when the

islanding detection program is activated, and the current waveform will be shifted 556  $\mu$ s. Fig. 13(b) shows the system is shut down after islanding occurred, and the detecting duration is about 308 ms. Finally, the highest efficiency of the high step-up DC-DC converter stage is about 96 %, and the measured system efficiency of the proposed micro inverter at full load operation is about 86 %.

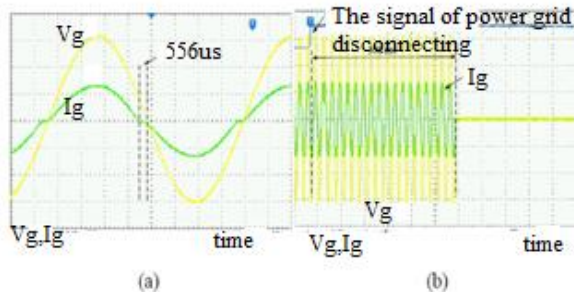


Fig. 13 . Measured waveforms of islanding detection. (a) Phase shift diagram when islanding detection program is activated. (b) System output voltage and current waveforms when the simulated power grid is cut off.

## V.CONCLUSION

A PV micro inverter has been designed, implemented and verified in this paper. The major difference between conventional PV inverter and the proposed micro inverter is the ability to raise the input voltage. The proposed micro inverter can efficiently raises the input voltage to the level that can be transformed to electricity. It also embedded with MPPT, system abnormal protection, and anti-islanding features; they are designed for harvesting maximum solar power from the PV module and preventing any abnormal situations occurred. The system abnormal protection and islanding detection are successfully activated and the system can be shut down within 1 second. The results are checked with simulation. Now a days in residential and industrial applications solar PV system which is gaining much more importance. So we have to find a better and efficient system for that we are using MPPT technique. In future grid connected system will become very common and solar PV system which gains much more important than other.

## REFERENCES

- [1] R. Ramaprabha, B. Mathur, M. Murthy, and S. Madhumitha, "New Configuration of Solar Photo Voltaic Array to Address Partial Shaded Conditions," *International Conference on Emerging Trends in Engineering and Technology*, pp. 328 - 333, 2010.
- [2] Q. Zhang, X. Sun, Y. Zhong, and M. Matsui, "A Novel Topology for Solving the Partial Shading Problem in Photovoltaic Power Generation System," *Power Electronics and Motion Control Conference*, pp. 2130 - 2135, 2009.
- [3] S. M. Chen, T. J. Liang, L. S. Yang, and J. F. Chen, "A Cascaded High Step-up DC-DC Converter with Single Switch for MicrosourceApplications," *IEEE Trans. Power Electron.*, vol. 26, no. 4, pp. 1146-1153, Apr. 2011.
- [4] T. J. Liang; S. M. Chen; L. S. Yang; J. F. Chen; Adrian Ioinovici, , "Ultra Large Gain Step-up Switched-Capacitor DC-DC Converter with Coupled Inductor for Alternative Sources of Energy," *IEEE Trans. Circuits Syst. I, Reg. Papers*, to be published.

- [5] T. J. Liang, S. M. Chen, L. S. Yang, J. F. Chen, A. Ioinovici, "A single switch boost-flyback DC-DC converter integrated with switched-capacitor cell," in *Proc. IEEE. ICPE & ECCE*, 2011, pp. 2782-2787.
- [6] W. Li and X. He, "Review of Non-isolated High-Step-Up DC/DC Converters in Photovoltaic Grid-Connected Applications" *IEEE Trans. Ind. Electron.*, vol. 58, no. 4, pp. 1239–1250, Mar. 2011.
- [7] T. H. Ai, J. F. Chen, and T. J. Liang, "A random switching method for HPWM full-bridge inverter," *IEEE Trans. on Ind. Electron.*, vol. 49, no. 3, pp. 595-597, Jun. 2002.
- [8] R. S. Lai and K.D.T. Ngo, "A PWM method for reduction of switching loss in a full-bridge inverter," *IEEE Trans. on Power Electron.*, vol. 10, no. 3, pp. 326-332, May 1995.
- [9] P. Midya, P. T. Krein, R. J. Turnbull, R. Reppa, and J. Kimball, "Dynamic maximum power point tracker for photovoltaic applications," in *Proc. IEEE PESC*, vol. 2, pp. 1710-1716, Jun. 1996. systems," in *Proc. IEEE IECON*, pp. 1073-1077, Nov. 1990.
- [10] J. H. R. Enslin, "Maximum power point tracking: a cost saving necessity in solar energy systems," in *Proc. IEEE IECON*, pp. 1073- 1077, Nov. 1990.
- [11] K. Harada and G. Zhao, "Controlled power interface between solar cells and AC source," *IEEE Trans. on Power Electron.*, vol. 8, no. 4, pp. 654-662, Oct. 1993.
- [12] R. Panda and R. K. Tripathi, "A novel sine wave inverter with PWM DC link," in *Proc. IEEE. ICIINFS*, pp. 1-5, Dec. 2008.

**First Author** Jinsa B Salim was born in Ernakulam. She received B-Tech degree from SNM IMT Engineering college in 2009, she is pursuing M-Tech from KMEA Engineering college, Kerala, India..

**Second Author.** Aabida C A Assistant Professor of KMEA Engineering college, received B-Tech from MES Engineering college Kuttipuram, M-Tech from BSA Crescent Engineering college Chennai, India